

The protection effectiveness of magnetite layers in relation to boiler corrosion

W.M.M. Huijbregts*, A. Snel*

5 th International Congress on Metallic Corrosion, Tokio, 1972,

* N.V. KEMA (joint laboratories electric utilities in The Netherlands) Utrechtseweg 310, Arnhem

Abstract

From failures in practical service and the results of exposure tests in small autoclaves as well as in an experimental 180 atm. boiler, it has become very clear, that not only the chemical water treatment but also the strength of the oxide layer must have an important influence on boiler corrosion.

Corrosion rates in hydroxide solutions were determined for chemically pure iron and several mild steel qualities. In the exposure tests a break-away in the oxidation curves was noticed. The pre-break-away parts of the oxidation curves could be described with a logarithmic oxidation equation, pointing to a mutual pore blocking mechanism and compressive growth stresses.

The tensile and compressive fracture strains of magnetite grown on mild steel appeared to be dependent on the hydroxide concentration, surface preparation of the samples and the kind of alkalizing chemical applied.

Defective tubes of operational boilers were examined very carefully. Three kinds of oxide scales were observed: very regular laminated, porous and blistered ones. The regular laminated scales can be explained as mainly a result of spalling of the oxide during the many shut-downs of boilers. The porous and blistered scales are considered to develop particularly at the operating temperatures as a result of compressive growth stresses.

1. Introduction

Water-side boiler corrosion in the power generation industry is generally a result of an unfavorable coincidence of heat flux, steam-water ratio, mass velocity, presence of deposits and water quality. Much work has already been done to study the influence of heat flux, steam-water ratios and mass transport on the tube temperature (1-6).

At about 5 to 10 % weight of steam the water is present as a thin film on the tube wall. In this film the heat transfer and boiling processes, like film, nucleate and columnar boiling, take place. In case of columnar boiling, oxide particles and corrosive salts will be deposited on the tube wall, resulting in pock-shaped deposits. Under such pocks pitting corrosion is often found (Figure 1).

The deposits generally consist of loose iron oxide, probably originated from the oxide layer at the tube walls elsewhere in the boiler.

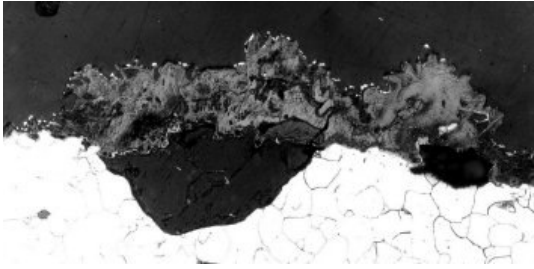


Figure 1. Pock shaped deposit and pitting, often noticed at places of columnar boiling.

1.1 Mechanism of oxide formation

The corrosion of iron and steel in concentrated hydroxide and chloride solutions has been studied extensively on the C.E.R.L. by Potter (7), Mann (8), Field (9), Harrison (10), Marsh (11) and Castle (12).

Field examined the possibility of adapting their measurements to a growth law, which was based on reasonable physical assumptions. In that case the oxidation of iron in 15% NaOH at 310 °C appeared to be controlled by a logarithmic oxidation law, based on the mutual pore blocking mechanism. For this mechanism the existence of "pores" in the oxide has been suggested, which will be blocked on account of compressive growth stresses in the oxide (Figure 2). As "pores" must be regarded any paths along which diffusion can occur at temperatures too low for lattice diffusion.

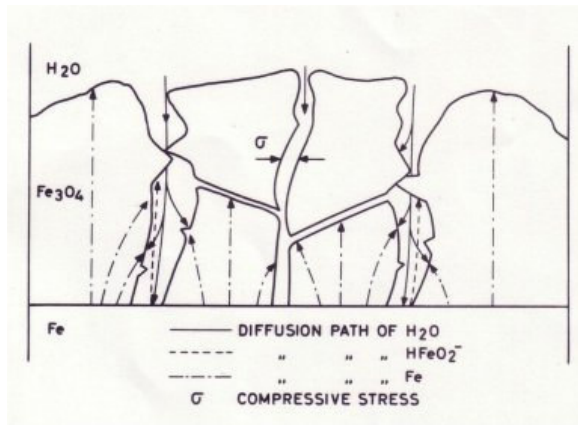


Figure 2. The pore blocking mechanism for the oxidation of iron in high temperature-pressure alkaline solutions.

Such diffusion paths could be axes of screw dislocations, grain boundaries, lines of edge dislocations, etc. In this oxidation mechanism the weight gain rate is proportional to the number of pores N , and the number of blocked pores is proportional to the density of the pores:

$$dx/dt = k_1 N \text{ and } dn = -k_2 N dx$$

From substitution of the number of pores N in the weight gain rate a logarithmic oxidation equation can be obtained:

$$x = 1/k_2 \ln (1 + k_1 k_2 N_0) \quad N_0: \text{ the number of pores at } t=0$$

Harrison (10) suggested that in the initial stage of oxide formation mutual pore blocking occurs, however at longer exposure times self pore blocking will be the rate controlling step, resulting respectively in a logarithmic and an asymptotic oxidation law. If, however, the compressive stresses become so large that the oxide will be cracked, new pores or microcracks are formed and a linear oxidation equation is obtained. It can be expected, that the three mechanisms mentioned will overlap each other.

2. Oxidation experiments

2.1. Experimental techniques

Samples of hard drawn and stress relieved chemically pure iron as well as of different mild steel qualities were used in the exposition tests. In table 1 the chemical analyses of these materials have been summarized.

Table 1 Chemical analyses of the specimen materials in %

| Specimen | Fe | C | Mn | Si | P | S | Mo |
|---|-------|------|------|------|-------|-------|------|
| Chemical pure iron; stress relieved; hard drawn | 99.95 | | | | | | |
| St. 35.8 | | 0.11 | 0.47 | 0.24 | 0.015 | 0.024 | |
| 14Mn4 | | 0.16 | 1.10 | 0.40 | 0.025 | 0.023 | |
| 15Mo3 | | 0.20 | 0.60 | | 0.32 | 0.016 | 0.29 |

Before exposure the finely revolved specimens were pickled in 10% HCL, water rinsed and dried with alcohol. The surface of each sample was 0,5 cm², The autoclaves, supplied with p.t.f.e, capsules were filled with 5 ml of the test solution. After the exposures the specimens were reduced in hydrogen atmosphere and weighed again. Loose oxide was only present in the exposure tests in weakly alkaline solutions. It was collected from the solutions by means of a magnet and analyzed in a Cahn R.G. thermo balance.

2.2. Exposure tests in solutions of different pH-values

To test the influence of pH on the oxidation rates some exposition experiments on iron in NaOH solutions at 300 °C were performed with an exposure time of 3 days. In figure 3 some of the results have been plotted, fig. At the lower pH values loose oxide was always present in the solutions. So in Figure 3 two graphs are given: the total weight gain as well as the weight gain of the adherent oxide plotted to the pH. The minimum weight gain was attained at a pH of 11.5. The loose oxide of the experiments at the pH values 9.0 and 9.5 was collected for X-Ray-diffraction. Only Fe₃O₄ was found.

2.3. Exposure tests in 0,01 n NaOH

Iron wires were corroded in deaerated 0.03 n NaOH at 310 °C (Figure 4).

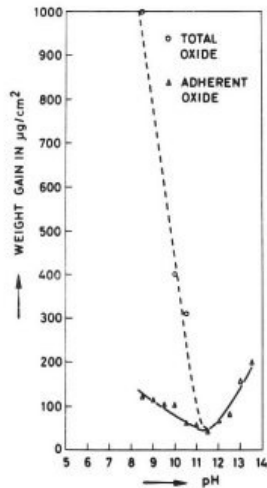


Figure 3. Weight gain of iron plotted to the pH value of the test solution; exposure time: 3 days.

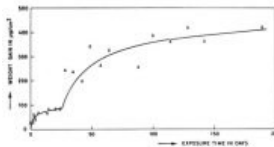


Figure 4 Oxidation rate of hard drawn iron in deaerated 0.03 n NaOH.

From this curve it is clear that initially a very regular growth of oxide a break-away after 25 days of exposure. The critical weight gain amounts to approximately $100 \mu\text{g}/\text{cm}^2$, corresponding with an oxide thickness of 0.8 microns. It is assumed that the magnetite has 15% porosity resulting in a specific weight of $4,5 \text{ gr}/\text{cm}^3$.

Such a breakaway was also found in the experiments on stress relieved iron in 0,01 n NaOH and LiOH. The break-away in the LiOH tests appeared to shift to higher weight gains and longer exposure times in relation to the NaOH experiments (Figure 5).

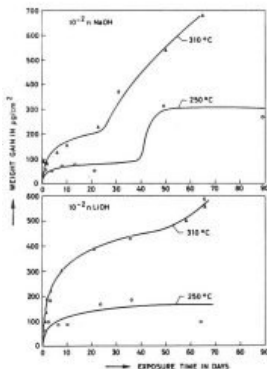


Figure 5. Oxidation of stress relieved iron in non-deaerated NaOH and LiOH; experiments no. 2 up to 5.

From the curves it was very clear that the oxide lost its protection effectiveness at a certain weight gain value. The wire samples of the tests presented in figure 4 were studied very intensively on the scanning electric microscope to detect cracks in the oxide. Only the post-break-away samples showed micro cracks in the compact initially protective magnetite layer (Figure 6).

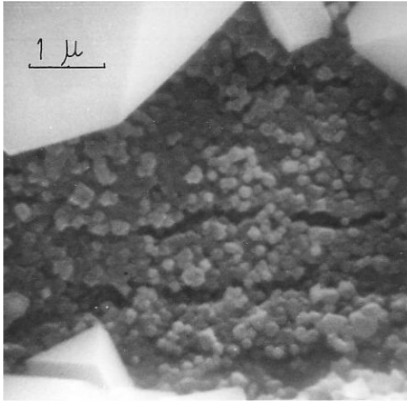


Figure 6. SEM picture of a post-break-away sample exposed in deaerated 0.03 NaOH at 310 °C.

Different boiler steel qualities were corroded in 0.01 n NaOH at 250 and 310 °C, The oxidation curves are summarized in Figure 7, from which it can be concluded that the oxidation rates of the three steels do not differ very much. In the experiments an obvious break-away could not always be detected.

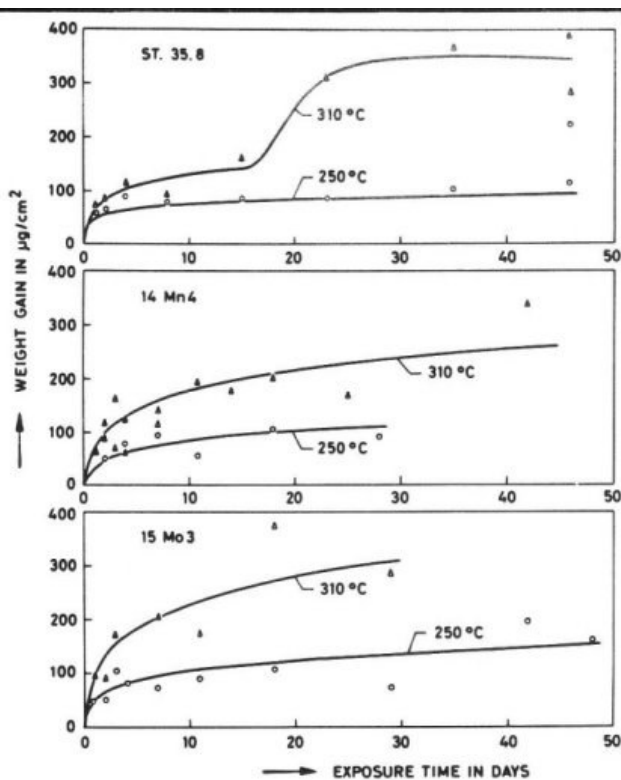


Figure 7. Oxidation rates of mild steel strips in non-deaerated 0.01 NaOH; experiments 6 up to 11.

Though the spread in the weight gains is rather high for drawing lines properly, it was tried to determine the oxidation equations to get more information about the oxidation mechanism. For this purpose the pre-break-away parts of the curves could be used. The appearance of a break-away itself, however, already gives some information about the mechanism. So the growth of the oxide must be considered to be attended with mechanical stresses, which will ultimately cause break of the oxide. This mechanism would be in agreement with the ideas of Field and Harrison, namely that the pore-blocking mechanism will take place, which implies the existence of compressive stresses in the oxide. Assuming that only mutual pore blocking will occur in the experiments, the factor $1/k_2$ and

$k_1k_2N_0$ could be determined by plotting weight gain to the logarithm of time. The factor $1/k_2$ was estimated from the slope of the line, and the term $1/k_2 \log k_1k_2N_0$ was given at $\log t=0$. In table 2 the oxidation equations, the factors k_1N_0 and the mechanical pore blocking parameters k_2 have been summarized.

Table 2 The oxidation parameters and the logarithmic equations.

| Exp. no | Specimen | Test solution | Temp. °C | k_1N_0 ug.day/cm ² | k_2 0.01cm ² /ug | Equation X:ug/cm ² T: day |
|---------|----------------------|-----------------------------------|----------|---------------------------------|-------------------------------|--|
| 1 | Hard drawn iron | Deaerated 0.03n NaOH 4 ppb Oxygen | 310 | 200 ± 10 | 2.3 ± 0.1 | X=44(log(1+4.6 t)) |
| 2 | Stress relieved iron | 0.01 n NaOH | 250 | 560 ± 340 | 3.3 ± 2 | X=30(log(1+19.0 t)) |
| 3 | | | 310 | 375 ± 30 | 0.91 ± 0.06 | X=110(log(1+3.4 t)) |
| 4 | | 0.01 n LiOH | 250 | 250 ± 100 | 1.4 ± 0.4 | X=75(log(1+3.5 t)) |
| 5 | | LiOH | 310 | 650 ± 6 | 0.47 ± 0.005 | X=215(log(1+3.1 t)) |
| 6 | St 35.8 | 0.01 n NaOH | 250 | 2680 ± 430 | 4 ± 0.5 | X=25(log(1+107 t)) |
| 7 | | NaOH | 310 | 455 ± 75 | 1.4 ± 0.2 | X=73(log(1+6.4 t)) |
| 8 | 14Mn4 | 0.01 n NaOH | 250 | 160 ± 80 | 1.7 ± 0.8 | X=59(log(1+2.7 t)) |
| 9 | | NaOH | 310 | 305 ± 95 | 0.80 ± 0.25 | X=126(log(1+2.4 t)) |
| 10 | 15Mo3 | 0.01 n NaOH | 250 | 345 ± 190 | 1.7 ± 1 | X=59(log(1+5.9 t)) |
| 11 | | NaOH | 310 | 525 ± 130 | 0.7 ± 0.2 | X=142(log(1+3.7 t)) |

The deviation in the factor $1/k_2$ was calculated from 2 the slopes of the two regression lines: weight gain as a function of log exposure time and log exposure time as a function of weight gain. The initial oxidation rates k_1N_0 at 310 °C are generally higher than the 250 °C values. The oxidation rates k_1N_0 in the experiments 2 and 6 appeared to be higher at 250 °C, which exposure tests could therefore be considered less reliable.

The mechanical pore blocking parameter, giving the rate of pore blocking, will particularly depend on the Pilling and Bedworth relation, the oxide growth in the micro pores, and the plastic flow or creep of the oxide. According to Stringer (13), plastic flow in growing oxide films will probably take place by creep and the most likely mechanisms are: dislocation climb, grain boundary sliding and Herring-Nabarro creep.

Dislocation climb and Nabarro creep require material transport by diffusion. At the relatively low temperature of 250 and 310 °C, lattice diffusion of iron can be neglected, so that the most likely mechanism for plastic flow in magnetite will be grain boundary sliding. If plastic flow does not take place the pores will not be blocked, but the oxide will probably crack ultimately on account of the increasing compressive growth stresses.

Though the deviations in the results are rather high, it can be concluded that the mechanical pore blocking parameter k_2 at 310 °C is approximately three times smaller than the 250 °C value, pointing to less pore blocking at the higher temperature. When oxidizing iron and mild steel at 250 °C, no obvious break-away was always found, indicating relatively low compressive stresses at 250 °C. The larger pore blocking parameter at 250 °C could be explained as a result of more grain boundary sliding, thus causing more stress relief and less compressive stresses. Besides, the oxide layer thickness at 250 °C is smaller than at 310 °C, which will also give less growth stresses and less chance of break off the oxide.

Applying LiOH instead of NaOH as an alkalizing chemical, smaller pore blocking parameters, but higher oxidation rates and break-away times were found. Magnetite grown in LiOH is coarser crystalline than the oxide formed in NaOH, giving less opportunity to grain boundary sliding and pore blocking.

2.4. Exposure tests in $10^{-5} n$ NaOH

When corroding iron and mild steel in weakly alkaline solutions a large divergence in the measurements was found. Nevertheless, several exposure tests in $10^{-5} n$ NaOH were performed to get a superficial idea of the corrosion resistance of various materials. The oxidation of 15Mo3 is given in Figure 8.

In Figure 9 the weight gains of several mild steels and iron, at longer exposure times at which the oxidation rate had become nearly constant, have been summarized in a histogram. Large differences in the corrosion resistance could not be stated for the various steels.

On account of the large divergence in the measurements no attempt was made to determine the suited oxidation equations.

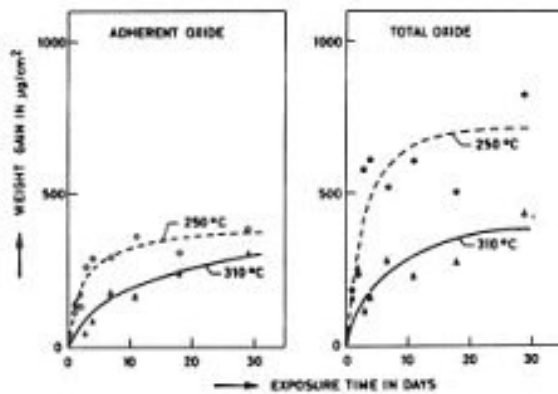


Figure 8. Oxidation rate of steel 15Mo3 strip in undeaerated $10^{-5} n$ NaOH.

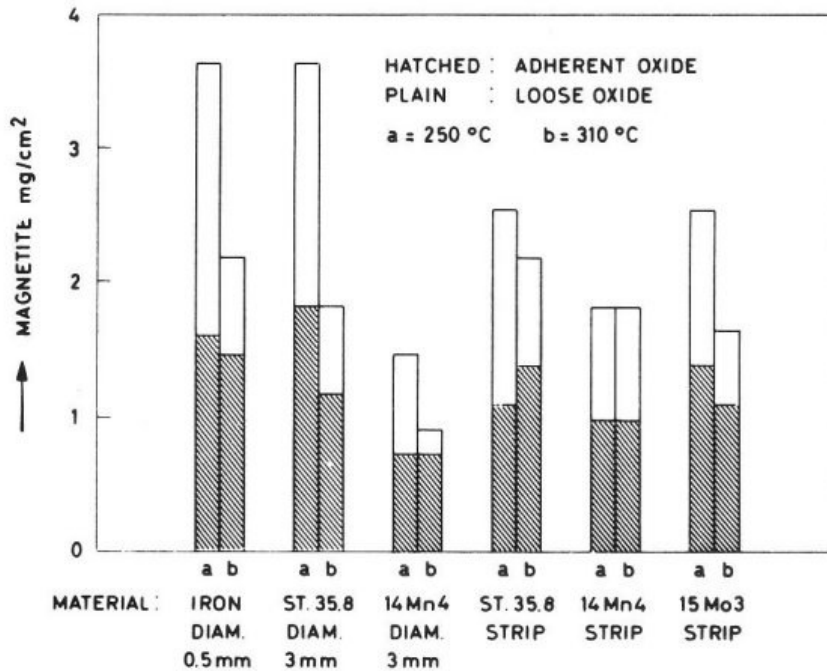


Figure 9. The amount of formed magnetite in non-deaerated $10^{-5} n$ NaOH at exposure times more than 30 days.

The results of these tests showed a smaller oxidation rate at 310° C compared with the one at 250° C, this in contrary to the experiments in 0,01 n hydroxide solutions.

The amount of loose oxide is generally larger at the 250° C experiments. Such an effect is only easily to understand assuming the loose oxide to be spalled from the samples on account of growth stresses. Consequently the growth stresses or strengths of magnetite at 310° C then should be smaller or larger respectively than those at 250° C. For a good understanding of boiler corrosion further research on this problem would be necessary.

3. Fracture-strains- of magnetite

From the results of the exposure tests it was obvious that the mechanical properties of the oxide will have a large influence on the protection effectiveness of the formed magnetite. In our experiments the fracture strains, tensile as well as compressive, were measured at room temperature on magnetite grown in 0,01 and 0,5 n NaOH and LiOH at 310° C. In the tensile strain experiments electrolytically polished as well as pickled samples were applied.

Magnetite grown in LiOH appeared to be coarser crystalline than the oxide formed in NaOH. The same effect was noticed when oxidizing polished or pickled samples and applying 0,5 or 0,01 n solutions.

To determine the tensile fracture strains, strains gauges were fixed on the partly pickled steel strips, which were installed in a simple straining apparatus. For the compressive strain experiments cylindrical steel samples (2.5 mm diam., 3 cm length) were applied.

These specimens were switched as working electrodes in a potentiostatic circuit. The tensile gauges were coated with an electrically isolated cement. The samples were kept at a potential of + 500 mV vs. S.H.E. in a chloride (500 mg/l) containing 0,01 n NaOH, during which the load was increased stepwise. As long as the oxide was intact the measured current was zero, but as soon as a small crack was formed a large current increase was noticed. The measured strain was regarded magnetite. The compressive fracture compressive strain in the cylindrical from the stress load and the Youngs modulus of steel (21.000 kg/mm²).

On account of differences in thermal expansion of the steel and magnetite, compressive strains in the oxide will occur at room temperature. The linear coefficient of thermal expansion for mild steel and magnetite (14) being $12,10 \cdot 10^{-6}$ and $8,46 \cdot 10^{-6}$ /°C respectively, the compressive strain when cooling the samples from 310 to 25°C will be 0,102%. Besides, compressive growth strains in the oxide could be present, this in accordance with the mutual pore blocking mechanism. Until now, however, these compressive growth strains were not yet determined.

Thus, to derive the fracture strains of magnetite only, the measured -tensile and compressive fracture strains of magnetite on steel at room temperature must be corrected at least with a compressive cooling strain of 0.102%. The results of the experiments have been listed in table 3.

Table 3 The fracture strains of magnetite at room temperature. Every value is the average of 4 measurements (accuracy 10%).

| Exposure time in days | Concentration | Steel quality | Tensile strains in % | | | |
|-----------------------|---------------|-----------------|--------------------------|-------|-----------|--------|
| | | | Measured | | Corrected | |
| | | | NaOH | LiOH | NaOH | LiOH |
| 12 | 0.01 n | 15Mo3 pickled | 0.174 | 0.188 | 0.072 | 0.086 |
| | | 14Mn4 pickled | 0.153 | 0.162 | 0.051 | 0.060 |
| | | St35.8 pickled | 0.148 | 0.182 | 0.046 | 0.080 |
| | | St35.8 polished | 0.122 | | 0.020 | |
| 12 | 0.5 n | St 35.8 pickled | 0.124 | 0.139 | 0.022 | 0.037 |
| | | St35.8 polished | 0.113 | | 0.011 | |
| | | | Compressive strains in % | | | |
| | | | Measured | | Corrected | |
| 12 | 0.01 n | St35.8 | 0.110 | 0.133 | 0.212 | 0.235 |
| 4 | 0.5 n | pickled | 0.120 | 0.134 | 0.222 | 0.0236 |

Though the mechanical properties of magnetite at room temperature will certainly differ from those at higher temperatures, the room temperature fracture strains will give a superficial idea about the qualities of different kinds of magnetite. A high alkalinity and electrolytically polishing of the samples resulted in lower tensile fracture strains. In these circumstances coarse crystalline magnetite is formed. Though the oxide grown in LiOH is coarser crystalline than the oxide formed in NaOH, this oxide had an obviously higher tensile fracture strain. Such an effect was also noticed, but to a less extent for the compressive fracture strains. According to Bloom and Jones (16), Li has been built in the spinel structure of magnetite. This appeared to have a favorable effect on the fracture strains. From the fracture strains in table 3 it is obvious that the steel quality 15Mo3 gives the better results, oxidizing both in NaOH and in LiOH.

4. Influence of compressive stresses at in-service failures

Besides the more fundamental research on magnetite formation, a lot of heavy corroded boiler tubes were examined very intensively. As already mentioned boiler corrosion is often a result of the coincidence of several unfavorable factors. It is likely that on-load corrosion is initiated by:

1. deposition of boiler sludge in which corrosive salts can be concentrated
2. columnar boiling, resulting in formation of pock shaped deposits under which pitting corrosion has been noticed very often
3. dry-out, attended by salt deposition and a high tube wall temperature
4. electrochemically pitting corrosion on account of a high corrosion potential (17).

However, once corrosion started, the oxidation can proceed very fast, and in our experience the on-load corrosion magnetite scales can be divided mainly into three characteristic types:

- a) a scale of very regular magnetite laminations (Figure 10)
- b) a scale of very porous magnetite (Figure 11)
- c) a scale of more irregular blistered oxide (Figure 12)



Figure 10. Regular laminated oxide in a heavy corroded boiler tube.

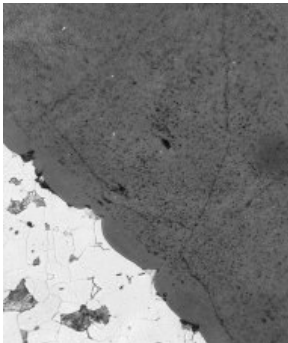


Figure 11. Porous oxide in a corroded boiler tube.

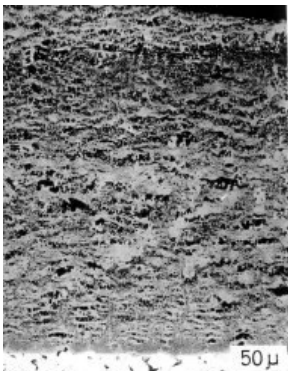


Figure 12. Blistered oxide in a corroded boiler tube.

In practice often a mixture of these three types can be found. We are of the opinion that these three types can be explained mainly from two different mechanism, namely:

1. scaling or detachment of the oxide on account of thermal stresses
2. break of magnetite as a result of compressive growth stresses

4.1 Failures by thermal stresses

As already discussed earlier temperature variations will give rather high compressive strains in the oxide layers. On places of large heat fluxes a dense, compact magnetite layer can be formed under operating conditions, which can be spalled easily when cooling the boiler tubes at shut-downs' thus resulting in a very regular laminated structure as shown in Figure 10. Failures of magnetite during shut-downs do not occur only in thick oxide scales but also in thin layers. At the KEMA laboratories St

35•8 tubes were exposed for two weeks in a 180 atm. experimental boiler at a steam water ratio of 0.7 and a heat flux of 200.000 kcal/m².h. By day the tubes were taken out of service every two hours. When examining the tubes many small red spots of Fe₂O₃ (hematite) were observed particularly on concave places as shown in Figure 13. On cooling the tubes the magnetite layer was cracked and the bare steel surface was rusted during the shut-down periods.



Figure 13. Dehydrated rust-layers on concave places of the rough boiler tubes. The rust has been formed during the many shutdowns.

4.2. Failures due to compressive growth stresses.

Besides the results of the oxidation experiments the appearance of thick porous and blistered magnetite scales in boiler tubes more or less confirmed the presence of these high compressive stresses. It is remarkable in Figures 11 and 12 that on the oxide metal interface a compact magnetite layer of about 1-2 μ thickness is present. Behind this layer some pores are noticed, which increase in number at longer distances from the metal oxide interface (Figure 14). Sometimes very thick porous, oxide layers were found as shown in Figure 11, but generally the porous oxide shades off into a blistered oxide structure (figures 12,14 and 15).

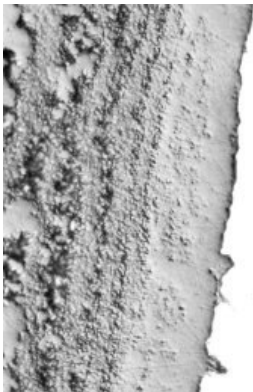


Figure 14. Corroded boiler tube. The numbers of pores increase at longer distances of the oxide-metal interface.

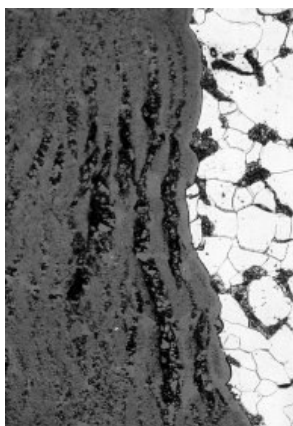


Figure 15. The compact layer of magnetite shades over into a porous or blistered structure.

When corroding mild steel samples in stainless steel autoclaves in 0,5 n NaOH at 360 °C, such blistered oxide layers were formed too, as shown in Figure 16. This oxide scale consists of 3 to 4 blistered magnetite layers.

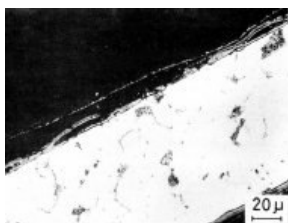


Figure 16. Blistered oxide formed in 0,5 n NaOH at 360 °C in an autoclave test.

The experiments were performed at a constant temperature, so that the blistered oxide layers can be considered to develop during the exposure and not when cooling the samples.

These typically porous and blistered oxides can be explained from the existence of compressive growth stresses in the oxide. The oxidizing medium, H₂O molecules, will migrate along the oxide grain boundaries, micro pores or other diffusion paths in the initially compact magnetite as was shown schematically in Figure 2. On account of increased oxide growth compressive stresses will increase, resulting in blocking of the diffusion paths. However, in case of insufficient plastic flow the oxide will ultimately crack, causing macro porosity. At increasing oxidation times the pores are supposed to act as notches for further cracking, and the micro cracks will increasingly gape by creep at longer times. From the results of the exposure tests at 360 °C, in which blistered oxide was grown, it can be concluded that magnetite is liable to plastic flow or creep under compressive stresses at the boiler operating tube wall temperature range of 350-450 °C. In practice the shut downs and thermal cycling will favor the blistering process very much.

Until now only the compressive stresses in the compact magnetite layers were discussed. However, high compressive strains can occur also in the coarse crystalline magnetite at the oxide-liquid interface. When corroding iron samples in 0,1 n NiCl₂ at 310 °C nickel was precipitated on the iron in the initial stage of the exposure, and on it large magnetite crystals are formed. This oxide growth appeared to be attended with such high stresses, that the magnetite layer and the nickel were undulated (Figure 17). Such an effect was also noticed in copper electroplated tubes, exposed in the experimental boiler which was operated with NaOH at a pH = 10,5.

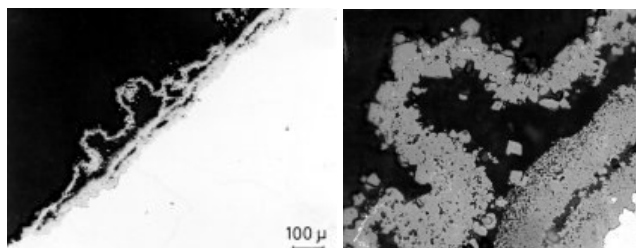


Figure 17. Iron, corroded in 0.1 n NiCl₂ at 310°C. Undulating oxide due to compressive growth stresses.

5. Conclusions

Though compressive growth stresses in magnetite have not yet been measured, the next phenomena very obviously point to the existence of these stresses:

1. The oxidation rates of iron and steel in 0,01 n NaOH and LiOH can be described with a logarithmic equation, based on a mutual pore blocking mechanism.
2. Formation of loose oxide in weakly alkaline solutions. This oxide breaks off from the samples during the exposure time.
3. Formation of pores and blisters in the oxide on tubes of operational boilers in case of heavy corrosion as well as on iron exposed in 0,5 n NaOH at 360 °C in an autoclave.
4. Undulating of coarse crystalline magnetite.

Fracture of magnetite can easily occur during shut-downs on account of the thermal stresses caused by differences in thermal expansion of magnetite and steel. Very regular laminated magnetite is a result of frequently taking the boiler out of service.

From our studies it seemed that the mechanical properties of magnetite will play an important role in boiler corrosion, because of deposition of the loose broken oxide on places of high heat fluxes. On account of the deposits and the proceeding corrosion the tube wall temperature will increase, which results in higher oxidation rates and higher compressive stresses. So, once corrosion has started, the formation of thick porous or blistered oxide will become more dependant on the oxidation temperature and the mechanical properties of magnetite than on the kind of corrosive salts, although the formation rate can be influenced by the water quality as is the experience in boiler corrosion practice.

Acknowledgements

We thank the Managing Board of the KEMA for its permission to publish the results of our research. Particular thanks are due to H.B.J. Klein-Avink, G.A.A. van Osch and P.H. Venderbosch for their dedication to the experimental work and to L.J. Elshout and J.A. de Nooyer for the many useful discussions.

References

1. P.R. Gilli, Mitt. V.G.B. 86, 288 (1963)
2. P. Pracht, Energie 10, 461 (1958)
3. R.K.F. Keeys, Report A.E.R.E.-R 64.11 (1971)
4. J.G. Collier, Nuclear Power 6, 61 (1961) . 7, 64.(1961)
5. D.W. Bell, Chem. Eng. Pro.-. 50, 449 (1954)
6. W.M.M. Huijbregts, Elektrotechniek 50, 195 (1972)
7. E.C. Potter, Chemistry and Industry 3, 308 (1959)
8. G.M.W. Mann, Chemistry and Indus-try 10, 1584 (1964)
9. E.M. Field, Proc. Sec. Intern. Congres on metallic corrosion, 829 (1966)
10. P.L. Harrison, Journ. Elect. Soc. 112, 235 (1965)
11. T.F. Marsh' Journ. Elect. Soc. 113? 313 (1966)
12. J.E. Castle, H.G. Masterson, Corrosion Science 6, 93 (1966)
13. J. Stringer, Corrosion Science 10, 513 (1970)
14. L. Rotherham, Joint intern. conference on creep New York, aug.

15. M.C. Bloom, Proc. symposium internal corrosion in boilers, Den Helder The Netherlands (1968)
16. R.L. Jones? Corrosion 27, 353 (1971)
17. W.M.M. Huijbregts, Mitt. V.G.B. 31 229 (1971)